Particle Filter Based Prognostics of PEM Fuel Cell in Bond Graph Framework

Mayank Shekhar JHA[#1], Mathieu Bressel[*&2],Belkacem Ould-Bouamama*[3]

Genevieve Dauphin-Tanguy[#4], Mickael Hilairet[&5], Daniel Hissel[&6]

[#]*CRIStAL UMR CNRS 9189, Ecole Centrale de Lille, Cité Scientifique 59650 Villeneuve d'Ascq France*

[*]*CRIStAL UMR CNRS 9189, Polytech Lille, Université de Lille 1, Cité Scientifique 59650 Villeneuve d' Ascq, France*

[&]*FEMTO-ST, UMR CNRS 6174, FCLAB, FR CNRS 3539, Rue Thierry Mieg, 90000 Belfort, France*

[1]jha.mayank.jha@gmail.com

[2]bressel.mathieu@gmail.com

[3]Belkacem.Ouldbouamama@polytech-lille.fr

[4]genevieve.dauphin-tanguy@ec-lille.fr

[5]mickael.hilairet@univ-fcomte.fr

[6]daniel.hissel@univ-fcomte.fr

***Abstract*— This paper develops an efficient solution towards the prognostics of industrial PEMFC. It involves an efficient multi-energetic model suited for diagnostics and prognostics, developed in Bond Graph framework. The benefits of Particle Filters (PF) is integrated with the BG model derived Analytical Redundancy Relations (ARRs), for prognostics of the electrical-electrochemical (EE) part. The prognostic problem is treated as the joint state-parameter estimation problem in Particle Filter framework, a hybrid prognostic approach wherein, a *fault model* is constructed in state-space. The state equation is inspired from the statistical degradation model of the global resistance and limiting current. Observation equation is obtained from the Analytical Redundancy Relations (ARRs) derived from BG model. Using PF algorithms, estimation of SOH is obtained along with the estimation of the associated hidden time-varying parameters that influence the progression of degradation. The latter is tracked to obtain the SOH in probabilistic terms. This in turn is used for prediction of Remaining Useful Life of the EE part of PEMFC. The methodology is applied on real degradation data sets under constant load current profile.**

***Keywords*— Prognostics, Bond Graph, Particle Filters, PEM Fuel Cell, Remaining Useful Life**

I. INTRODUCTION

The presence of irreversible degradation severely affects the useful life of PEMFC and leads to inefficiency, reduced lifespan, lesser power density and high maintenance cost [1]. This issue is best addressed when approached from the perspective of Prognostic and Health Management (PHM)[2].

There are very few existing model-based works that propose efficient prognostic solutions for PEMFC. [3] proposes physics based Degradation Model (DM) of the Electro-Chemical Active Surface Area (ECSA), used for damage tracking and prediction using Unscented Kalman Filter. [4] proposed the method employing statistical log-linear Degradation Model (DM) and Particle Filters (PF) for estimation of State of Health (SOH) estimation and Remaining Useful Life (RUL) prediction. The DM used therein lacks the insight into the physics of the phenomenon.

Bond Graph modelling technique has been extensively used owing to the behavioural, structural and causal properties[5], that provide a systematic approach towards development of supervision and fault detection and Isolation (FDI) of highly non-linear and complex thermo-chemical systems [6-8]. In BG framework, the model based FDI is mainly based upon ARRs [9-11]. For deterministic systems, the properties and ARR generation algorithm are well detailed in [9].

Hybrid prognostic approaches [12, 13] combine the advantages of the model based approaches [2] and data-driven prognostics [14]. Here, physics or statistical based DMs are employed and measured information is used to adapt the estimation of damage progression.

Specifically, PF algorithms has been exploited very widely for prognostics of incipient parametric degradation in the system. Here, the prediction of the RUL is obtained as probability distribution which accounts for the various involved uncertainties[15, 16]. Significant works include assessment of the end of discharge and RUL in lithium-ion batteries [17], battery health monitoring [18], estimation and prediction of crack growth[19], application to pneumatic valve[15], estimation-prediction of wear as in centrifugal pumps[16], assessing uncertainty management options for prognostics [20], etc. Comprehensive studies of various optimal or sub-optimal filters for prognostic purposes are found in [21-23].

This paper develops a novel and efficient solution towards the prognostics of PEMFC. The issue of modeling of the complex and energetically mutually-dependent dynamics of PEMFC, is tackled in Bond Graph (BG) framework. The

second issue of prognostics is addressed for the electrical-electrochemical (EE) part. The prognostic problem is cast as the joint state-parameter estimation problem in Particle Filter (PF) framework, a hybrid prognostic approach wherein, a *fault model* is constructed in state-space. The state equation is inspired from the statistical degradation model of the global

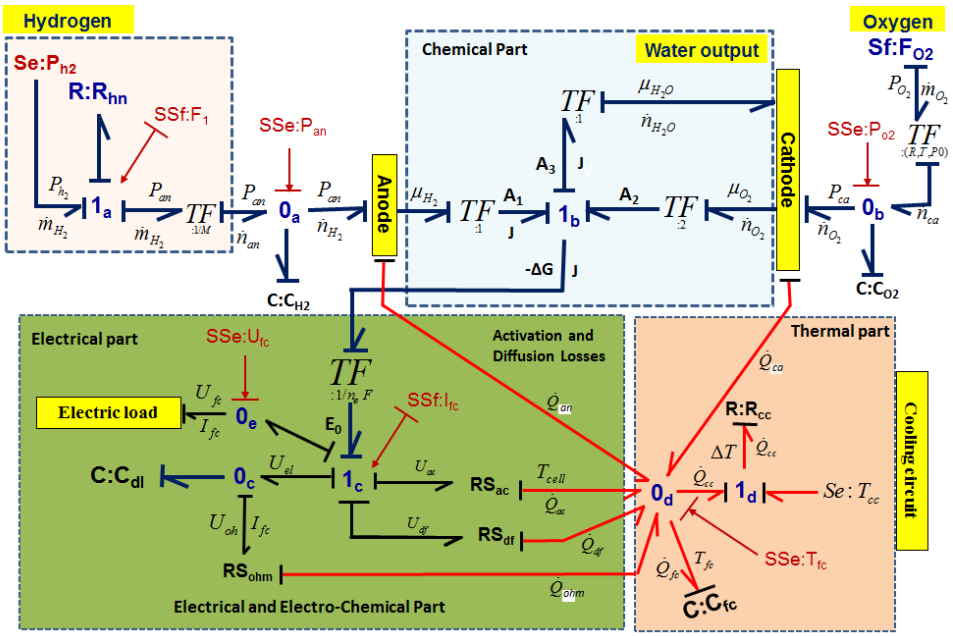

Fig. 1 Bond graph model of the PEMFC in preferred derivative causality

resistance and limiting current. Observation equation is obtained from the Analytical Redundancy Relations (ARRs) derived at the EE subsystem of the BG model. Using PF algorithms, estimation of State of Health (SOH) is obtained along with the estimation of the associated hidden time-varying parameters that influence the progression of degradation. The estimations are achieved in probabilistic terms. This in turn is used for prediction of RUL of the EE part of PEMFC. The methodology is applied on real degradation data sets under constant current load profile.

II. BG Model of PEMFC

The extensively developed basic chemistry of PEMFC is omitted in this paper and can be found in [24]. Instead, on the physical level, the developed BG model of the global system is presented in Fig. 1. The global system is decomposed into various subsystems where the input and output for each, are the exchanged powers represented by two conjugated power variables: effort and flow (graphically shown by a half-arrow). Derivative causality (suited for diagnostic and prognostic) is preferred, compared to the integral causality (close to the reality of physics, suited for simulation purposes). This helps in avoiding unknown initial condition problem for ARR generation. All detectors (*De* for the effort detector and *Df* for the flow detector) are *dualized* into sources of signal *SSe* and *SSf* respectively used as inlet nodes in the unknown variable elimination oriented graph [10].

In this paper, focus remains on EE subsystem only and thus, details of modeling, ARR generation etc. is provided for the same, exclusively. Modeling details of the global model is not presented descriptively.

Source of hydrogen is represented by $\mathrm{Se}:P_{H_2}$ where the corresponding pressure P_{H_2}, is a known quantity. The valve represented by a resistive BG element $\mathrm{R}:Rh_n$ (where sub-script n denotes the nominal value) regulates the flow of hydrogen (measured by $SSf:F_{H2}$). The pressure on the anode compartment is measured by the pressure sensor $SSe:P_{an}$. The hydraulic dynamics (storage of gases) is represented with the capacitive elements $\mathrm{C}:C_{H2}$ for anode. To transform the mass flow (kg/s) into a molar flow (mole/s), a transformer element $\underset{:1/M}{TF}$ is used where M is the modulus representing the molar mass (kg/mole). Flow sensor $SSf:F_{H2}$ measures the mass flow rate $\dot{m}_{H_2}$. The three transformer elements therein, $\underset{:\nu_i}{TF}(i=1,2,3)$, have their respective modulus ν_i, that represent the stoichiometric coefficients of the reactants ($\nu_1=1$ for hydrogen and $\nu_2=2$ for oxygen) and the product water with $\nu_3=1$.

The EE subsystem accounts for electrical part and activation-diffusion losses. The kinetics of reduction-oxidation reaction (in chemical part, not detailed here) generates an over-voltage which is termed as activation loss. Furthermore, the resistivity of the membrane electrode assembly decreases the operational potential due to the Ohmic effect. The resistance value depends on the degree of humidification of the membrane and on the temperature. Finally, species are consumed and imply a loss of partial pressure on the reaction surfaces, thereby reducing the Nernst

potential significantly especially at high currents. This phenomenon is called diffusion / concentration losses. Moreover, during transients, electron accumulation along the membrane electrode interface is observable. It is the double layer capacitance effect.

In the BG model, the EE subsystem and the chemical part are connected using the transformer. This results in obtaining the thermodynamic potential as,

$$E_0 = -\frac{\Delta G}{n_e F} = -\frac{A_1 + A_2 - A_3}{n_e F} = \frac{\mu_{H2} + \frac{1}{2}\mu_{O2} + \mu_{H2O}}{n_e F} \quad (1)$$

where R is the perfect gas constant, μ_x is the chemical potential of species x and the water is in liquid phase, where n_e is the number of electrons involved in the reaction and F is the number of Faraday. Moreover,

$$\begin{aligned} \mu_{H2} &= \mu_0^{H2} + RT_{H2}\ln\left(P_{H2}\right) \\ \mu_{O2} &= \mu_0^{O2} + RT_{O2}\ln\left(P_{O2}\right) \\ \mu_{H2O} &= \mu_0^{H2O} \end{aligned} \quad (2)$$

RS is an active two port dissipative (resistive) element that generates thermal energy. The two port thermal dissipative element RS_{ohm} models the Ohmic losses (membrane, electrodes and connectors). Similarly, the activation and the diffusion phenomenon are modelled by RS_{ac} and RS_{df} respectively. The associated power variables are related as,

$$U_{ac} = AT\ ln\left(\frac{I_{fc}}{I_0}\right) \quad (3)$$

$$U_{df} = BT\ ln\left(1 - \frac{I_{fc}}{I_L}\right) \quad (4)$$

where, A is the activation constant $A = R/\chi nF$; and B is the diffusion constant; $B = -RT/\chi nF$ with χ as the transfer coefficient, I_0 is the exchanged current, I_{fc} is the load current and I_L is the limiting current i.e. maximal current the fuel cell is able to provide. The double layer capacitance phenomenon is modeled by a capacitor element $C : C_{dl}$ and imposes the dynamics of the activation phenomena. U_{el} is expressed at the junction $\mathbf{0_C}$, as the solution of the equation:

$$I_{fc} = \frac{U_{el}}{R_{ohm}} + C_{dl}\frac{dU_{el}}{dt} \quad (5)$$

where R_{ohm} is the global resistance (membrane and connectors).

III. Derivation of Determinist ARR

In BG context, ARR is a constraint expression being a function of system parameters and known variables as,

$$ARR : f(SSe, SSf, Se, Sf, MSe, MSf, \boldsymbol{\theta}) \quad (6)$$

Here, the ARR is generated from the $\mathbf{1_c}$ junction which deals with the energetic assessment of EE subsystem. It is termed as ARR_2.

$$ARR_2 : n_s\left(E_0 - U_{ac} - U_{df} - U_{el}\right) - U_{fc} = 0 \quad (7)$$

where n_s is number of cells in a stack. From (1)-(4), the unknown variables can be eliminated using causal paths and known electro-chemical relations such that, ARR_2 is expressed as,

$$\begin{aligned} ARR_2 = n_s &\left(\begin{array}{l} \mu_0^{H2} + RT_{H2}\ln\left(P_{H2}\right) + \frac{1}{2}\left[\mu_0^{O2} + RT_{O2}\ln\left(P_{O2}\right)\right] \\ -\mu_0^{H2O} - R_{ohm}I_{fc} - ATln\left(\frac{I_{fc}}{I_0}\right) - BTln\left(1 - \frac{I_{fc}}{I_l}\right) \end{array} \right) \\ &- SSe : U_{fc} \\ = n_s &\left(E_0 - R_{ohm}I_{fc} - AT\ln\left(\frac{I_{fc}}{I_0}\right) - BT\ln\left(1 - \frac{I_{fc}}{I_L}\right)\right) \\ &- SSe : U_{fc} \end{aligned} \quad (8)$$

Note that due to fast electrical dynamics (5) has been approximated as:

$$U_{el} = R_{ohm}.I_{fc} \quad (9)$$

ARR_2 is sensitive to drying, flooding and aging of the fuel cell and forms the main attraction of the paper.

IV. Degradation Model

Periodically, throughout the life of the fuel cell, the static response is measured with a polarization curve (voltage as a function of the current). The BG derived ARR of (8) represents the polarisation curve. The degradation test was performed for about 800 hours, on a commercially available stack of 5 cells, surface of 100 cm² and a nominal constant current load $I_{nom} = I_{fc}$ of 70A. For each of the characterization times, a Levenberg-Marquardt method is used to extract the parameters of (9). The algorithm is initiated with a set of parameters whose values are chosen from the literature [24, 25]. The algorithm extracts: the Open Circuit Voltage (OCV) E_0 at nominal pressure and temperature, the global resistance R_{ohm} (membranes, connectors, end plates, etc.), the exchange current I_0 and the limiting current I_L.

Tthe recorded stack voltage U_{fc} (at sampling period of one hour) is shown in Fig. 2. The resulting model fitting of the measured polarization curves (during aging) is shown in Fig. 3. Fig. 4 shows the evolution of the parameter value with respect to the initial one (in percentage). From the four chosen parameters, only two show significant deviations: the overall

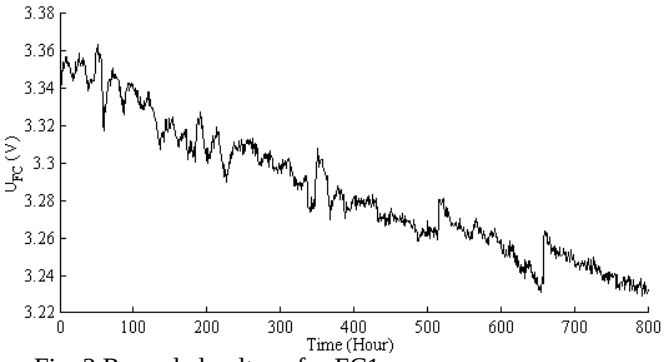

Fig. 2 Recorded voltage for FC1

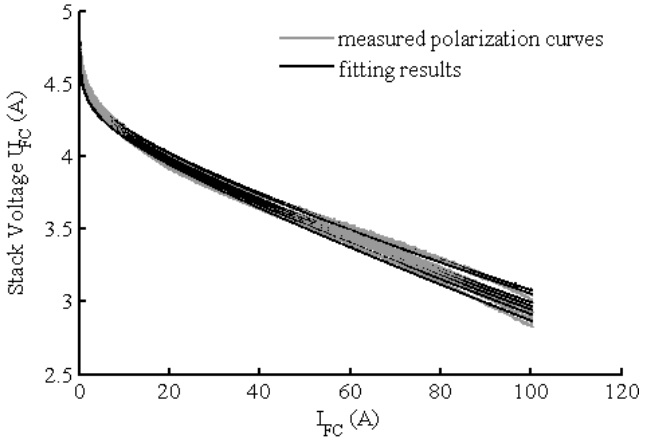

Fig. 3 Polarization Curve and fitting result during ageing for FC1

resistance R_{ohm} increases by more than 12% while the limit current I_L decreases by 13%.

For a given operating condition, since only the stack voltage is measured, it is impossible to separate the mutual coupling of global resistance and limiting current i.e. the loss due to both are not observable simultaneously. Therefore, the variations in the latter are parameterized with a single parameter α , a State of Health (SOH) indicator. The variation is expressed in form of linear equation (since the parameters value seems to follow a linear variation) as,

$$\begin{aligned} R_{ohm}(t) &= R_{ohm,n}\left(1+\alpha(t)\right) \\ I_L(t) &= I_{L,n}\left(1-\alpha(t)\right) \\ \alpha(t) &= \beta \times t \end{aligned} \tag{10}$$

where β explains the approximately constant rate-change of α and sub-script *n* denotes the nominal value. Very recently in [26], this approach is proposed for construction of state equation.

V. The Hybrid Prognostic Methodology

The methodology involves construction of the fault model of the degradation candidates: R_{ohm} and I_L . The state equation is inspired from the statistical degradation model of (10). Since their state can be indicated by the state of $\alpha(t)$ and the associated hidden factor $\beta(t)$, $\alpha(t)$ forms the degradation candidate and $\beta(t)$ is the degradation progression parameter (DPP). Observation equation is obtained from the nominal ARR. Then, PF is used for joint estimation of state (SOH) and hidden parameter DPP. *Sampling Importance Resampling* (SIR) PF is employed for estimation and it is not described here. It can be found detailed in [27].

A. Fault Model Construction

In discrete time step $k \in \mathbb{N}$, the fault model can be described in stochastic framework as,

$$\begin{aligned} \alpha_k &= \alpha_{k-1} + \beta_{k-1} \times \Delta t + v_{k-1} \\ \beta_k &= \beta_{k-1} + \xi_{k-1} \end{aligned} \tag{11}$$

$$y_k^d = h_k^d\left(\alpha_k, \beta_k\right) + w_k^d \tag{12}$$

where, $v_k \sim \mathcal{N}(0, \sigma_v^2)$ is the associated process noise $\xi_k \sim \mathcal{N}(0, \sigma_\xi^2)$ is a random walk noise , Δt is the sample time, y_k^d is the observation equation, $h(.)$ is any non-linear function of state variables and $w_k^d \sim \mathcal{N}(0, \sigma_{w^d}^2)$ is the measurement noise.

Measurements y_k^d are assumed conditionally independent, given the state process. The likelihood function becomes as,

$$p\left(y_k^d \mid \alpha_k^d, \beta_k^d\right) = \frac{1}{\sigma_{w_k^d}\sqrt{2\pi}} \exp\left(-\left(y_k^d - h^d\left(\alpha_k^d, \beta_k^d\right)\right)^2 \Big/ 2\sigma_{w_k^d}^2\right) \tag{13}$$

The measurement of the state health can be obtained implicitly from the nominal part of $ARR_2 : r_{2,n}(t)$, which is exploited to obtain the observation equation as:

$$r_2(t) = r_{2,n}(t) + n_s\left(\begin{array}{l} -R_{ohm,n}\alpha(t)I_{fc} - BT\ ln\left(1-\dfrac{I_{fc}}{I_{L,n}\left(1-\alpha(t)\right)}\right) \\ +BT\ ln\left(1-\dfrac{I_{fc}}{I_{L,n}}\right) \end{array}\right) = 0 \tag{14}$$

Thus, measurement of $\alpha(t)$ is acquired from $r_{2,n}(t)$ .In discrete time *k*, observation equation is,

$$y^d(k) = r_{2,n}(k) = n_s\left(\begin{array}{l} R_{ohm,n}\alpha_k I_{fc} + BT\ ln\left(1-\dfrac{I_{fc}}{I_{L,n}\left(1-\alpha_k\right)}\right) \\ -BT\ ln\left(1-\dfrac{I_{fc}}{I_{L,n}}\right) \end{array}\right) + w_k^d \tag{15}$$

where $w_k^d \sim \mathcal{N}(0, \sigma_{w^d}^2)$ models the noise associated with measurement acquisition and is approximated as Gaussian in nature. σ_{w^d} is approximated from residual measurements during degradation tests.

B. SOH Estimation and RUL Prediction

PF algorithm used to estimate the SOH and DPP is tabulated in Table I. wherein, $\left\{(\alpha_{k-1}^{i}, \beta_{k-1}^{i}), \mathrm{w}_{k-1}^{i}\right\}_{i=1}^{N}$ denotes the particle i, w_{k-1}^{i} denotes the weight of the latter and N is the number of particles.

Table I

Joint SOH and DPP Estimation

Algorithm 1: Estimation using SIR filter

Inputs: $\left\{(\alpha_{k-1}^{i}, \beta_{k-1}^{i}), \mathrm{w}_{k-1}^{i}\right\}_{i=1}^{N}$, y_k^d

Output: $\left\{(\alpha_k^{i}, \beta_k^{i}), \mathrm{w}_k^{i}\right\}_{i=1}^{N}$

for i**=1 to N do**

$\beta_k^{i} \sim p(\beta_k^{i} \mid \beta_{k-1}^{i})$

$w_k^i \sim p(y_k^d \mid \alpha_k^i, \beta_k^i)$

end for

$W \leftarrow \sum_{i=1}^{N} w_k^i$

for i**=1 to N do**

$w_k^i \leftarrow w_k^i / W$

end for

$\left\{(\alpha_k^{i}, \beta_k^{i}), \mathrm{w}_k^{i}\right\}_{i=1}^{N} \leftarrow \mathrm{RESAMPLE}\left\{(\alpha_k^{i}, \beta_k^{i}), \mathrm{w}_k^{i}\right\}_{i=1}^{N}$

The RUL prediction is done by projecting each of the particles that constitute the estimation, into future (l steps ahead) till the estimated state reaches its pre-fixed failure state α_{fail} [4, 15, 16, 28]. The estimation of the state and RUL prediction step form one single iteration step. The RUL prediction algorithm is given in Table II.

Table II

RUL Prediction

Algorithm 2: RUL Prediction using PF

Inputs: $\left\{(\alpha_k^{i}, \beta_k^{i}), \mathrm{w}_k^{i}\right\}_{i=1}^{N}$

Variable: l

Outputs: $\left\{RUL_k^{\alpha^i}, \mathrm{w}_k^{i}\right\}_{i=1}^{N}$

for i=1 **to** N **do**

l**=0**

while $\alpha_{k+l}^{i} \le \alpha_{fail}$ **do**

$\beta_{k+1}^{i} \sim p(\beta_{k+1}^{i} \mid \beta_k^{i})$

$\alpha_{k+1}^{i} \sim p(\alpha_{k+1}^{i} \mid \alpha_k^{i}, \beta_{k+1}^{i})$

$l \leftarrow l+1$

end while

$RUL_k^{\alpha^i} \leftarrow l$

end for

C. Evaluation Metrics

Metrics employed for assessment of the prognostic performance is briefed here. They are found detailed in [29] and case study implementing the same is found in [16, 28].

Root mean square error (RMSE): This metric expresses the relative estimation accuracy as:

$$\mathrm{RMSE}_X = \sqrt{Mean_k\left[\left(\frac{mean(X) - X^*}{X^*}\right)^2\right]} \tag{16}$$

where, for species X, X^* denotes the corresponding true values. $Mean_k$ denotes the mean over all values of k. For a particular prediction time point k_p, the prediction accuracy is evaluated by relative accuracy (RA) metric as,

$$\mathrm{RA}_{\alpha,k_p} = \left(1 - \frac{\left|RUL^*_{\alpha,k_p} - \mathrm{Median}\, p(RUL_{\alpha,k_p})\right|}{RUL^*_{\alpha,k_p}}\right); \tag{17}$$

$$\overline{\mathrm{RA}}_{\alpha} = \mathrm{Mean}_{k_p}\, p(\mathrm{RA}_{\alpha,k_p}) \tag{18}$$

The overall accuracy is determined by $\overline{\mathrm{RA}}_{\theta^d}$ .The metric: $\alpha - \lambda$ [29], is employed to summarize the prognostic performance where $\alpha \in [0,1]$ defines the bounds of true *RUL* as $(1 \pm \alpha) RUL^*_{\alpha,k_p}$. It should not be confused with SOH indicator $\alpha(t)$.

D. Results and Discussion

Motivated from Fig. 4, $\alpha_{fail} = 0.12$ signifies end of life of at 12% deviation on initial value. Moreover, α_{true} is considered to evolve in a perfect linear way with true value of slope β , $\beta_{true} = 1.3 \times 10^{-4}$ such that α_{fail} is reached at 900 hours. Also, measurement variance: $\sigma^2_{w^d} = 10^{-6}$. Estimation performance by PF as shown in Fig. 5, is realized with N=2000 particles, $\sigma^2_{\xi} = 10^{-10}$, $\sigma^2_{v} = 10^{-6}$. Therein, the approximately linear α is estimated with $RMSE_{\alpha} = 23.56\%$ and the approximately constant β is estimated accurately with $RMSE_{\beta} = 9.3\%$. Fig. 6 shows the box plot of RUL predictions obtained at time interval of 25 hours (for the sake of clarity). For all time points, prediction performance is assessed by α-λ metric with α=0.4 and β=0.4 . The latter translates to the requirement: containment of 40% of RUL probability mass within 40% of true RUL value. Percentage of probability mass falling within the accuracy cone is indicated against each box plot. Starting from t=200 hours, almost all the predictions are *true* (acceptable), except the ones at the last four prediction-points. This arises mainly because of characterizations performed at t=800 hours such that insufficient recovery effect happens on the stack voltage while the latter is recorded. Over all, starting from t= 350 hours, the prediction performance is very accurate with $\overline{\mathrm{RA}} = 96.07\%$.

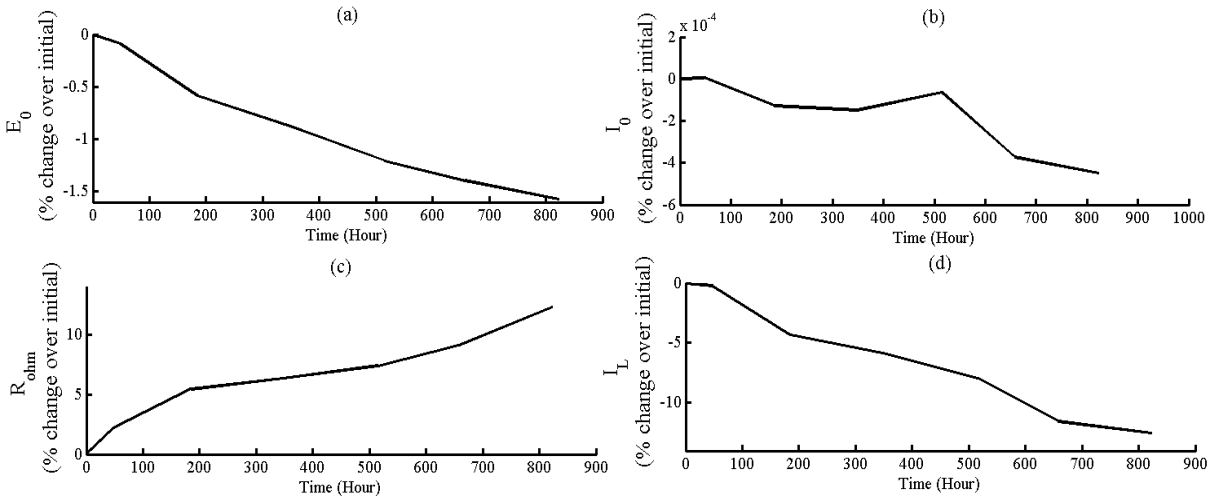

Fig. 4 Deviation of the parameters values (in percentage of their initial value) during aging: (a) Change in E_0, (b) Change in I_0, (c) Change in R_{ohm} (d) Change in I_L

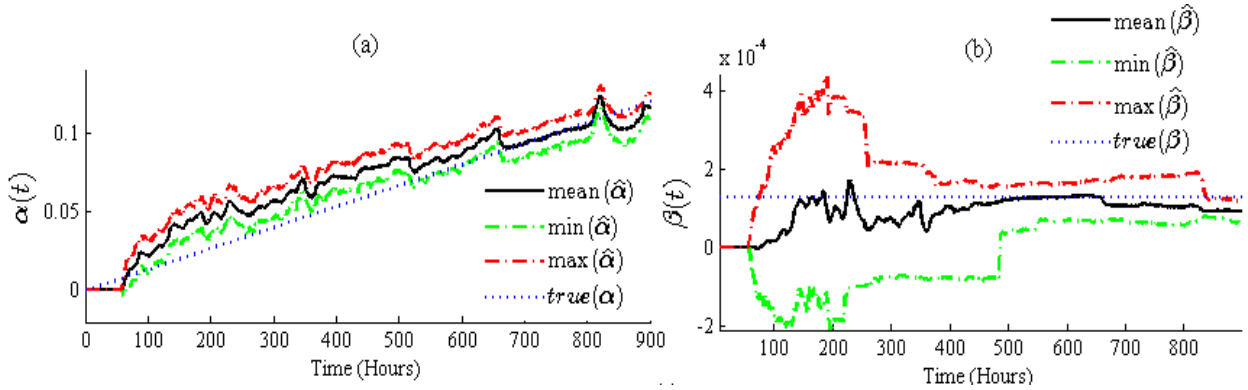

Fig. 5 Estimation performance in PF for FC1 (a). Estimation of α (b) Estimation of β

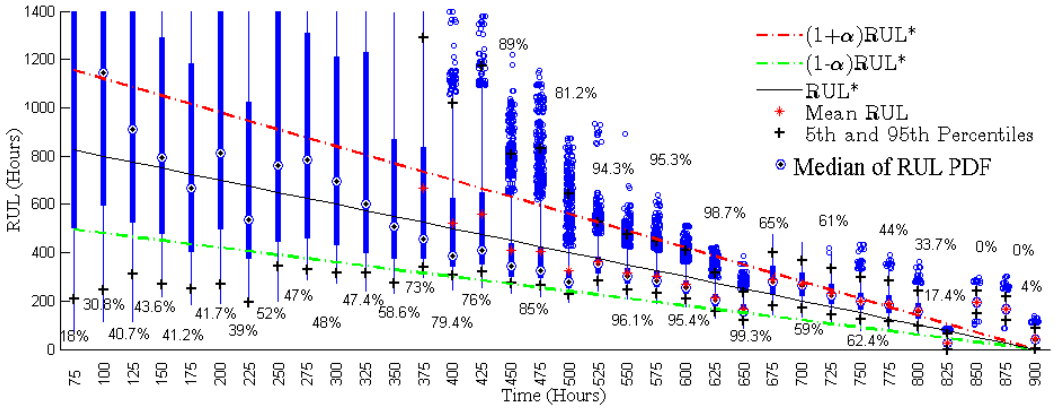

Fig. 6 RUL Prediction

VI. Conclusions

Through real degradation data sets, the proposed methodology is able to successfully assess the SOH and predict the RUL with a very high accuracy and precise confidence bounds. The proposed methodology thus, exploits the benefits of BG and PF for an efficient functional decomposition of PEMFC and accurate SOH estimation and RUL prediction. Using the same approach, the developed model can be used for prognostics of

other sub-systems (hydraulic, thermal etc.) with the availability of degradation data. The latter forms a potential future work. Moreover, the methodology applied here on PEMFC, has the potential to be applied over any multi-energetic system. Also, authors have explored the same approach over the degradation tests where the current load is variable. The obtained results can be discussed in an extended version of the paper. The accuracy of results obtained here demonstrates the viability of the method for prognostics.

ACKNOWLEDGMENT

This work was supported by the project ANR PROPICE (ANR-12-PRGE-0001) and by the project LABEX ACTION (ANR-11-LABX-01-0) both funded by the French National Research Agency.

REFERENCES

[1] X. Luo, J. Wang, M. Dooner, and J. Clarke, "Overview of current development in electrical energy storage technologies and the application potential in power system operation," *Applied Energy*, vol. 137, pp. 511-536, 2015.

[2] A. K. Jardine, D. Lin, and D. Banjevic, "A review on machinery diagnostics and prognostics implementing condition-based maintenance," *Mechanical systems and signal processing*, vol. 20, pp. 1483-1510, 2006.

[3] Y. Wang, K. S. Chen, J. Mishler, S. C. Cho, and X. C. Adroher, "A review of polymer electrolyte membrane fuel cells: technology, applications, and needs on fundamental research," *Applied Energy*, vol. 88, pp. 981-1007, 2011.

[4] M. Jouin, R. Gouriveau, D. Hissel, M.-C. Péra, and N. Zerhouni, "Prognostics of PEM fuel cell in a particle filtering framework," *International Journal of Hydrogen Energy*, vol. 39, pp. 481-494, 2014.

[5] A. Mukherjee and A. K. Samantaray, *Bond graph in modeling, simulation and fault identification*: IK International Pvt Ltd, 2006.

[6] K. Medjaher, A. K. Samantaray, B. Ould Bouamama, and M. Staroswiecki, "Supervision of an industrial steam generator. Part II: Online implementation," *Control Engineering Practice*, vol. 14, pp. 85-96, 1// 2006.

[7] R. Kumar and L. Umanand, "Modeling of a pressure modulated desalination system using bond graph methodology," *Applied Energy*, vol. 86, pp. 1654-1666, 9// 2009.

[8] M. Tan, L. Chen, J. Jin, F. Sun, and C. Wu, "Bond-graph-based fault-diagnosis for a marine condensate–booster–feedwater system," *Applied Energy*, vol. 81, pp. 449-458, 8// 2005.

[9] B. O. Bouamama, A. Samantaray, M. Staroswiecki, and G. Dauphin-Tanguy, "Derivation of constraint relations from bond graph models for fault detection and isolation," *SIMULATION SERIES*, vol. 35, pp. 104-109, 2003.

[10] A. K. Samantaray and B. O. Bouamama, *Model-based process supervision: a bond graph approach*: Springer Science & Business Media, 2008.

[11] M. Jha, G. Dauphin-Tanguy, and B. Ould Bouamama, "Robust FDI based on LFT BG and relative activity at junction," in *Control Conference (ECC), 2014 European*, 2014, pp. 938-943.

[12] J. Sikorska, M. Hodkiewicz, and L. Ma, "Prognostic modelling options for remaining useful life estimation by industry," *Mechanical Systems and Signal Processing*, vol. 25, pp. 1803-1836, 2011.

[13] G. Vachtsevanos, F. Lewis, M. Roemer, A. Hess, and B. Wu, *Intelligent Fault Diagnosis and Prognosis for Engineering Systems*. New Jersey: John Wiley & Sons, Inc., 2007.

[14] M. Schwabacher, "A survey of data-driven prognostics," in *Proceedings of the AIAA Infotech@ Aerospace Conference*, 2005, pp. 1-5.

[15] M. J. Daigle and K. Goebel, "A Model-Based Prognostics Approach Applied to Pneumatic Valves," *International Journal of Prognostics and Health Management*, vol. 2, 2011.

[16] M. J. Daigle and K. Goebel, "Model-based prognostics with concurrent damage progression processes," *Systems, Man, and Cybernetics: Systems, IEEE Transactions on*, vol. 43, pp. 535-546, 2013.

[17] B. Saha and K. Goebel, "Modeling Li-ion battery capacity depletion in a particle filtering framework," in *Proceedings of the annual conference of the prognostics and health management society*, 2009, pp. 2909-2924.

[18] B. Saha, K. Goebel, S. Poll, and J. Christophersen, "Prognostics methods for battery health monitoring using a Bayesian framework," *Instrumentation and Measurement, IEEE Transactions on*, vol. 58, pp. 291-296, 2009.

[19] E. Zio and G. Peloni, "Particle filtering prognostic estimation of the remaining useful life of nonlinear components," *Reliability Engineering & System Safety*, vol. 96, pp. 403-409, 2011.

[20] P. Baraldi, F. Mangili, and E. Zio, "Investigation of uncertainty treatment capability of model-based and data-driven prognostic methods using simulated data," *Reliability Engineering & System Safety*, vol. 112, pp. 94-108, 4// 2013.

[21] D. An, N. H. Kim, and J.-H. Choi, "Practical options for selecting data-driven or physics-based prognostics algorithms with reviews," *Reliability Engineering & System Safety*, vol. 133, pp. 223-236, 2015.

[22] M. Daigle, B. Saha, and K. Goebel, "A comparison of filter-based approaches for model-based prognostics," in *Aerospace Conference, 2012 IEEE*, 2012, pp. 1-10.

[23] B. Saha, K. Goebel, and J. Christophersen, "Comparison of prognostic algorithms for estimating remaining useful life of batteries," *Transactions of the Institute of Measurement and Control*, 2009.

[24] J. Larminie, A. Dicks, and M. S. McDonald, *Fuel cell systems explained* vol. 2: Wiley New York, 2003.

[25] E. Laffly, M.-C. Péra, and D. Hissel, "Polymer electrolyte membrane fuel cell modelling and parameters estimation for ageing consideration," in *2007 IEEE International Symposium on Industrial Electronics*, 2007.

[26] M. Bressel, M. Hilairet, D. Hissel, and B. Ould-Bouamama, "Extended Kalman Filter for Prognostic of Proton Exchange Membrane Fuel Cell," *Submitted to Applied Energy*, 2015.

[27] M. S. Arulampalam, S. Maskell, N. Gordon, and T. Clapp, "A tutorial on particle filters for online nonlinear/non-Gaussian Bayesian tracking," *Signal Processing, IEEE Transactions on*, vol. 50, pp. 174-188, 2002.

[28] M. Daigle and K. Goebel, "Model-based prognostics under limited sensing," in *Aerospace Conference, 2010 IEEE*, 2010, pp. 1-12.

[29] A. Saxena, J. Celaya, B. Saha, S. Saha, and K. Goebel, "Metrics for offline evaluation of prognostic performance," *International Journal of Prognostics and Health Management Volume 1 (color)*, p. 4, 2010.